

Excitation of the $n=4$ Levels of He^+ by the Impact of H^+ , He^+ and He^{2+} Ions

By

Masatoshi ASARI*, Akio ITOH* and Fumio FUKUZAWA*

(Received September 21, 1981)

Abstract

The emission cross sections of HeII ($4 \rightarrow 3$) 4686 Å line by the incident beams of 0.5–1.5 MeV H^+ , 1.0–2.5 MeV He^+ and 1.0–2.0 MeV He^{2+} are studied. By measuring the lateral distribution of the light intensity, the excitation of He^+ ($n=4$) levels is found to be caused by direct collision. The emission cross section by the proton impact is due to the "ionization process" and shows an E^{-1} dependence, while that by the helium ion impact is due to the "charge transfer process" as well as the "ionization process" and shows a steeper energy dependence.

1. Introduction

The experimental study of the excitation of a gaseous target by the impact of fast charged particles is very important for the fundamental understanding of the complex phenomena of atomic collisions. Recently, many investigations on atomic collisions with a spectroscopic technique have been reported. This technique is one of the most useful means for obtaining information on the excited states of ions, atoms and molecules. The results of the measurement can give emission cross sections, and moreover, excitation cross sections when the branching ratios of the corresponding transitions are exactly known. This kind of work, up to 1970, has been reviewed by Thomas.¹⁾ The present work confines the investigation to the excitation of the $n=4$ levels of He^+ by proton and helium ion impacts.

There are several reports²⁻⁹⁾ on the excitation of the $n=4$ levels of He^+ by electron impact. In this case, the excitation of He^+ takes place via simultaneous ionization and excitation:



In the case of proton impact, it is possible that the electron in the target helium transfers to the projectile, and the following two processes must be taken into

* Department of Nuclear Engineering.

account:



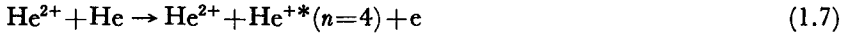
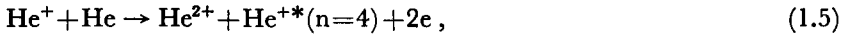
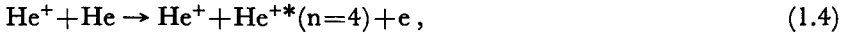
and



Usually, the former process is called the "ionization process" and the latter the "charge transfer process".

In Mapleton's papers, the theoretical excitation cross sections via the "ionization process" are given up to the $n=3$ He^+ levels¹⁰⁾, and those via the "charge transfer process" up to the $n=2$ He^+ levels.¹¹⁾ However, there is no theoretical estimation of excitation cross sections for the formation of the $n=4$ He^+ levels. The experimental studies on the simultaneous ionization and excitation of helium by proton impact have been reported by several investigators.^{5,12-16)} Most of the measurements were made with proton energies below 200 keV. Only Thomas' work was made in the comparable energy region with our present work.

For helium ion impact, there are many possibilities for making a simultaneous "ionization and excitation of target helium:



and



The processes (1.4), (1.5) and (1.7) are the "ionization process" and others are the "charge transfer process". There is no experimental nor theoretical work on these processes.

In the present work, the emission cross section of the HeII ($4 \rightarrow 3$) 4686 Å line emitted from a helium gas target was measured. For the incident beams 0.5–1.5 MeV H^+ , 1.0–2.5 MeV He^+ and 1.0–2.0 MeV He^{2+} ions were used. The beam current was about 5 μA for the He^+ and He^{2+} incidences, and 1 μA for the proton incidence for all the measurements of the present work.

In order to obtain sufficient light intensities with these incident beam currents, it is necessary to use somewhat higher target pressures. In the present experiment, we measured the light emitted from a point 10 cm downstream from the entrance slit of the differentially pumped target cell. For the helium ion incidence, therefore, the effect of charge-changing collisions in the gas target must

be taken into account. That means the impact of both He^+ and He^{2+} ions must be considered, even if either He^+ or He^{2+} ion is used as the incident beam. From the measurements of the pressure dependence of the emission cross sections for the primary incident beams of He^+ and He^{2+} , the emission cross sections for $\text{He}^+ + \text{He}$ collisions and those for $\text{He}^{2+} + \text{He}$ collisions can be determined separately.

2. Experimental Method and Apparatus

The experimental arrangement is shown schematically in Fig. 1. The ion

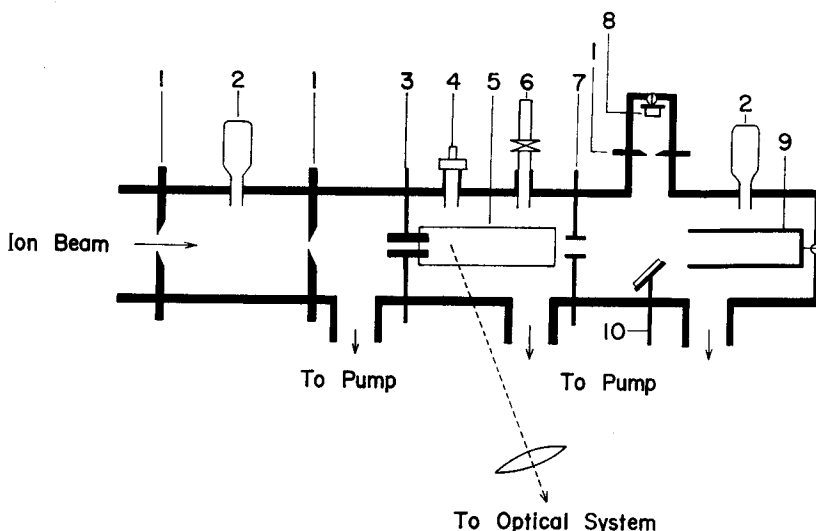


Fig. 1. Schematic experimental arrangement: 1) collimating slit, 2) ionization vacuum gauge, 3) entrance slit, 4) Pirani gauge, 5) quartz window, 6) gas inlet, 7) exit slit, 8) SSD, 9) Faraday cup, 10) movable Ta plate.

beam from a Van de Graaff accelerator was passed through a target cell which was about 50 cm in length. The entrance slit of the target cell was 2 mm in diameter and 30 mm in length, and had a threaded inner surface for suppressing the edge scattering. The exit slit was 4 mm in diameter and 20 mm in length. Two kinds of beam-monitoring systems were used for different experimental purposes. One is a Faraday cup, and the other a Solid-State-Detector (SSD), which detects 90 deg.-scattered particles from a thick Ta plate placed in front of the Faraday cup. This Ta plate was mounted on a movable target holder and was moved away from the beam course when the Faraday cup was used. The output signal of the Faraday cup system is independent of the projectile energy and mass, but depends on the projectile charge. However, that of the SSD system has just the reverse dependence. Therefore, the SSD is suitable when the pressure de-

pendence of the emission cross section is measured, as well as when the emission cross sections between He^+ and He^{2+} incidences are compared. On the contrary, the Faraday cup is rather suitable when the energy dependence of the emission cross section is measured, as well as when the emission cross sections between the proton and helium ion incidences are compared.

In order to deduce the particle flux from the Faraday cup reading, it is necessary to make corrections for the charge fractions of the beam. Charge fractions were measured for the He^+ and He^{2+} incidences on the He target, and are shown in Figs. 2(a)-(b).¹⁷⁾ These charge fractions are in good agreement with the calculated

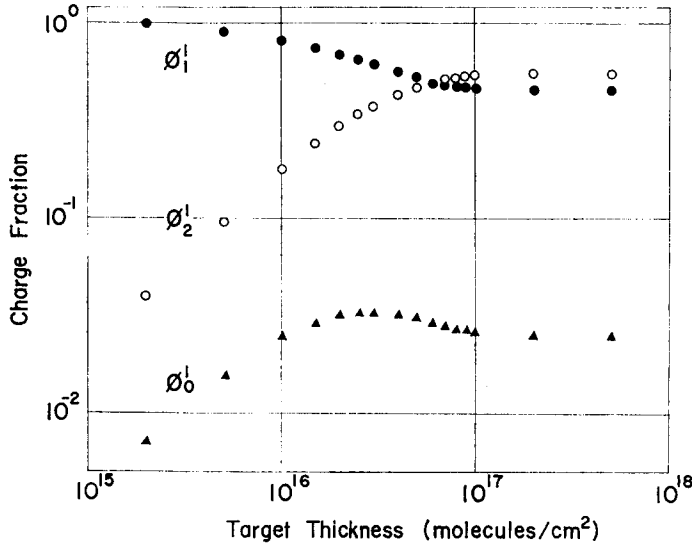


Fig. 2(a). Charge fractions of 1.0 MeV He^+ incidence on He.

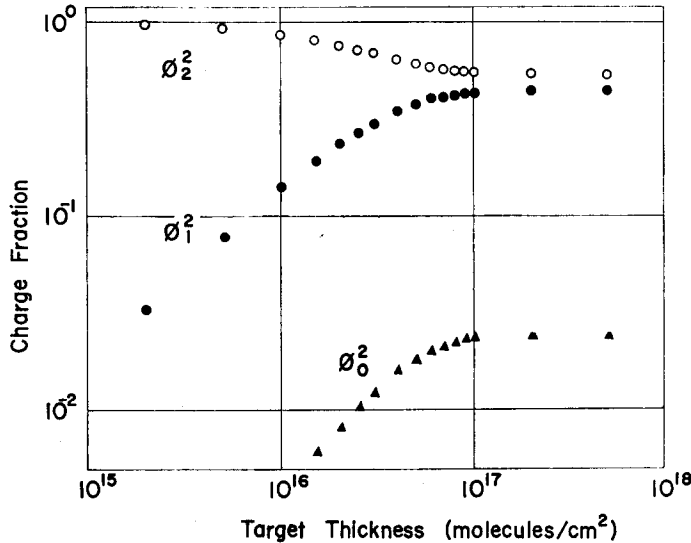


Fig. 2(b). Charge fractions of 1.0 MeV He^{2+} incidence on He.

values based on the published experimental charge-changing cross sections.¹⁸⁻²¹⁾

The emitted radiations from the excited target ions were measured through a quartz window of the target cell. They were focused by a quartz lens and were analyzed with a monochromator in conjunction with a photomultiplier. The optical system was set at an angle of 65 deg. with respect to the beam direction. This arrangement made it easy to distinguish between the emitted radiation from an excited target helium ion and that from an excited projectile helium ion. In Fig. 3 is shown the spectrum resulting from the 1.0 MeV He^+ incidence on He.

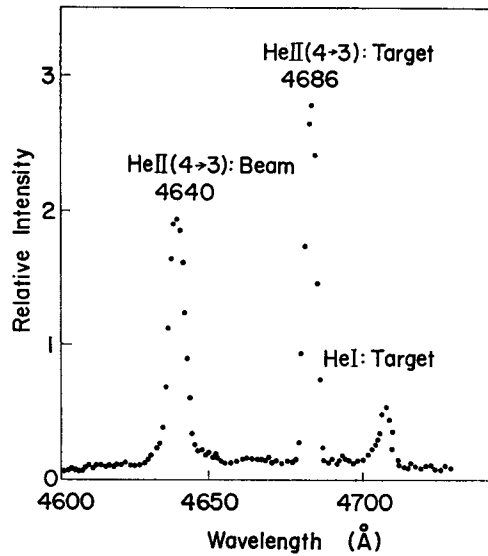


Fig. 3. Spectrum produced by 1.0 MeV He^+ incidence on He at a target pressure of 0.03 Torr.

The radiation in the transition He^+ ($4 \rightarrow 3$) is observed as the 4686 Å line when it is emitted from the excited target He^+ ion. Because of the Doppler effect, the line is shifted to 4640 Å when it is emitted from the excited projectile He^+ ion.

3. Results and Discussions

In order to confirm that the excitation of the $n=4$ levels of He^+ was caused by the direct collision between a projectile ion and a target atom, the lateral distribution of the light intensity of 4686 Å line was measured. The lateral distribution means the variation of the light intensity along the axis perpendicular to the beam direction. In the previous works, we studied the lateral distribution for some collision processes, and obtained the following results²²⁻²⁴⁾. The lateral distribution for the direct collision had a sharp peak around the beam axis, and that for

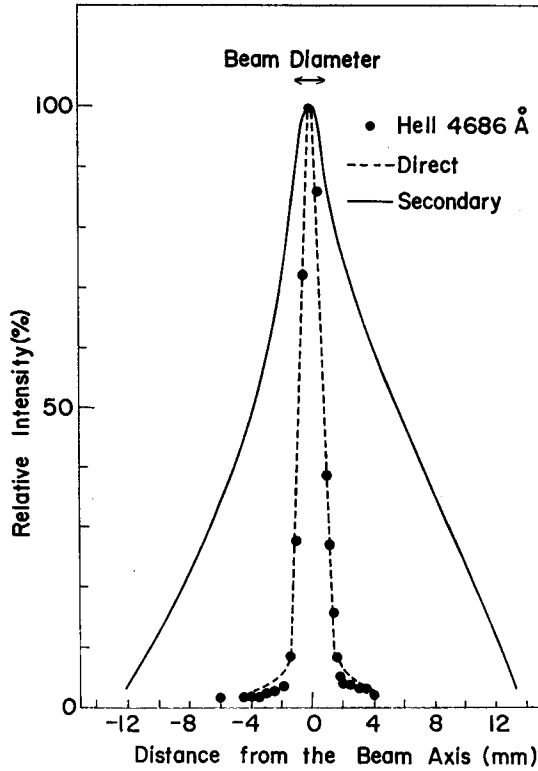


Fig. 4. Lateral distribution of the light intensity of HeII 4686 Å line. Solid line (N_2 3371 Å) and dashed line (N_2^+ 3914 Å) are experimental curves by the impact of 150 keV proton on N_2 gas.

the secondary electron collision had a broad distribution. In Fig. 4 is shown the lateral distribution of the 4686 Å line resulting from the 1.0 MeV He^+ incidence on He. Also shown are typical distributions for a direct collision and for a secondary electron collision. The present lateral distribution is in good agreement with that of the direct collision. This leads to the conclusion that the formation of the $n=4$ levels of He^+ is caused by a direct collision.

For the direct collision process, the intensity of the emitted light as well as the density of excited atoms is proportional to the target density ρ . When the ions in charge state k and energy E enter the target cell, the intensity of the light I^k at the distance l downstream from the entrance slit is given by

$$I^k = \rho \sum_q \Phi_q^k(\rho l, E) \sigma_q(E), \quad (3.1)$$

where, $\Phi_q^k(\rho l, E)$ is the beam flux of ions in charge state q . $\sigma_q(E)$ is emission cross section for a collision between a target atom and a colliding ion in charge state q .

$\Phi_q^k(\rho l, E)$ is the product of the total beam flux Φ^k and the fraction of charge state q at the distance l , $\phi_q^k(\rho l, E)$, that is,

$$\Phi_q^k(\rho l, E) = \Phi^k \phi_q^k(\rho l, E) . \quad (3.2)$$

Substituting eq. (3.2) into eq. (3.1), we obtain:

$$I^k = \rho \Phi^k \sigma^k(x, E) , \quad (3.3)$$

where $x = \rho l$,

$$\sigma^k(x, E) = \sum_q \phi_q^k(x, E) \sigma_q(E) . \quad (3.4)$$

The quantity $\sigma^k(x, E)$ is hereafter called the effective emission cross section.

In the case of helium ion incidence, the pressure dependence of the effective emission cross sections $\sigma^1(x, E)$ and $\sigma^2(x, E)$ was measured in a pressure range from 0.003 to 1.0 Torr at the incident energies of 1.0, 1.5 and 2.0 MeV. The measured charge fractions show that the maximum of $\phi_0^k(x, E)$ is below 0.04 in these energies. Therefore, the term with $q=0$ on the right hand side of eq. (3.4) is neglected, and the effective emission cross sections for the He^+ and He^{2+} incidences are given by the following expressions:

$$\sigma^1(x, E) = \phi_1^1(x, E) \sigma_1(E) + \phi_2^1(x, E) \sigma_2(E) \quad (3.5)$$

and

$$\sigma^2(x, E) = \phi_1^2(x, E) \sigma_1(E) + \phi_2^2(x, E) \sigma_2(E) . \quad (3.6)$$

When the above equations are used directly for estimating $\sigma_1(E)$ and $\sigma_2(E)$ with the experimental values of $\sigma^1(x, E)$ and $\sigma^2(x, E)$, the results have large errors caused by the following situations.

(1) Errors in the pressure measurement propagate directly to the experimental values of $\sigma^1(x, E)$ and $\sigma^2(x, E)$.

(2) In the higher pressure region, the effect of the beam-divergence results in the large values of $\sigma^1(x, E)$ and $\sigma^2(x, E)$.

(3) Because of the small but significant difference in the beam courses of the He^+ and He^{2+} incidences, there are some differences in the efficiency of the beam flux monitor and in the solid angle of the light detection.

In order to improve the analysis, we used the ratio $\sigma^1(x, E)/\sigma^2(x, E)$ in the wide pressure range, and $\sigma^1(x, E)$ at the relatively higher target pressure instead of $\sigma^1(x, E)$ and $\sigma^2(x, E)$. By this ratio, there are cancellations of errors originating from the situations (1) and (2). In Fig. 5, the ratio $\sigma^1(x, E)/\sigma^2(x, E)$ is plotted as a function of the target pressure. In the higher pressure region, we should have a ratio of unity because the equilibrium charge state distribution must be

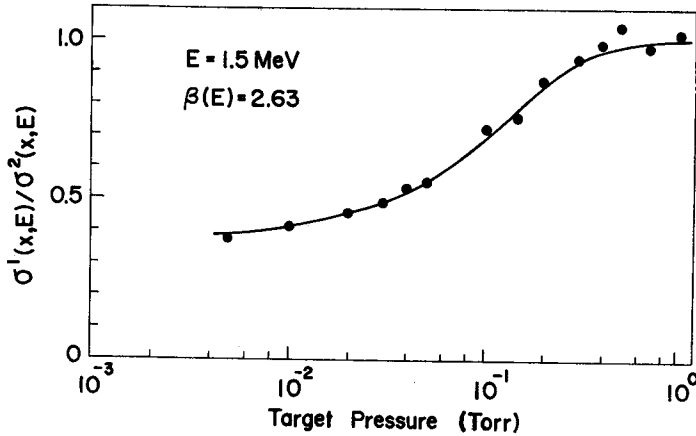


Fig. 5. Corrected ratio $\sigma^1(x, E) / \sigma^2(x, E)$ as a function of He gas pressure at $E = 1.5$ MeV. Solid line is obtained by the least square fitting of eq. (3.7) to these points with $\beta(E) = 2.63$.

established. However, due to the situation (3), the above ratio was different from unity. A correction must be made so as to make a ratio unity in the higher pressure region. Corrected data points are shown by the full circles in Fig. 5.

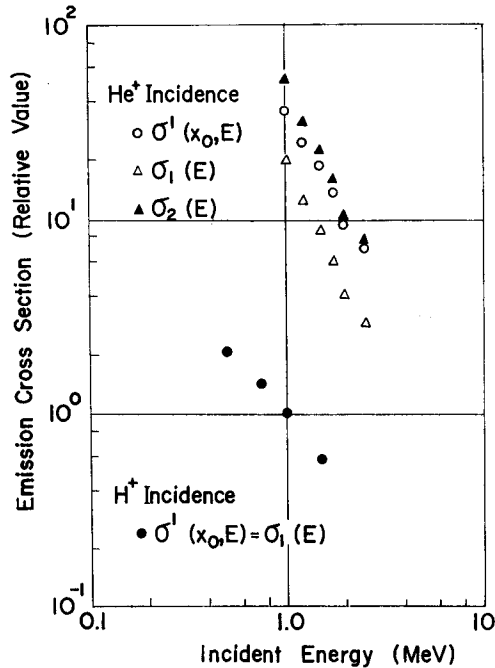


Fig. 6. Measured effective emission cross section $\sigma^1(x_0, E)$ and estimated emission cross sections $\sigma_1(E)$ and $\sigma_2(E)$. The x_0 corresponds to the target pressure of 0.15 Torr.

The ratio $\sigma^1(x, E)/\sigma^2(x, E)$ is related to $\sigma_2(E)/\sigma_1(x, E) \equiv \beta(E)$ as follows:

$$\frac{\sigma^1(x, E)}{\sigma^2(x, E)} = \frac{\phi_1^1(x, E) + \beta(E)\phi_2^1(x, E)}{\phi_1^2(x, E) + \beta(E)\phi_2^2(x, E)}. \quad (3.7)$$

By the least square fitting of eq. (3.7) to the corrected data points, the value of $\beta(E)$ can be obtained. The solid line in Fig. 5 is the calculated one with the most probable value of $\beta(E)=2.63$. It is in excellent agreement with the corrected data points over the wide pressure region. At other energies, namely 1.0 and 2.0 MeV, similar results were obtained. Considering the uncertainties in charge fractions due to experimental errors in pressure measurement, we obtained 2.6 ± 0.3 as the value of $\beta(E)$ in the present energy region.

In Fig. 6 are shown the effective emission cross sections and the estimated emission cross sections by proton and He^+ incidences at the relatively higher target pressure of 0.15 Torr. For the helium ion incidence, by using the above value of

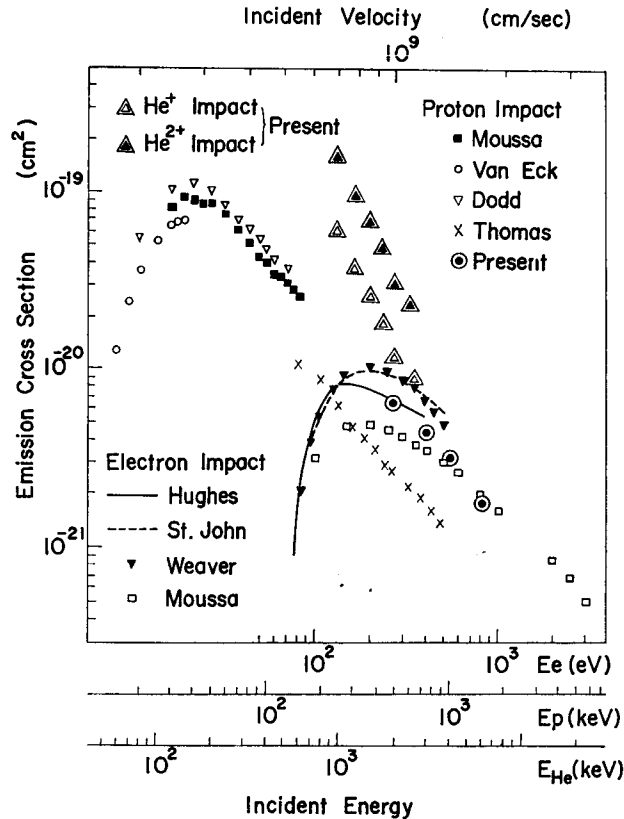


Fig. 7. Emission cross section of HeII (4→3) as a function of incident energy. E_e , E_p and E_{He} represent the energies of electron, proton and helium ions, respectively.

ratio $\beta(E)$ and the equilibrium charge fractions, we estimated $\sigma_1(E)$ and $\sigma_2(E)$. For the proton incidence, the neutral fraction is negligibly small (less than 10^{-3}) in the present energy region, and $\sigma_1(E)$ is almost equal to $\sigma^1(E)$.

In Fig. 7 are compared the emission cross sections by electron, proton, He^+ and He^{2+} impacts with the same velocities. The normalization of our data was made so that the emission cross section at the proton energy of 500 keV was 6.5×10^{-21} cm². It can be seen in this figure that our data with this normalization lies on the straight line extrapolated from the proton data by Moussa and De Heer⁵⁾. It also agrees with their electron data at relatively high velocities. It should be noted that all the experimental emission cross sections by proton impact have the same energy dependence ($\propto E^{-1}$) above the energy of 60 keV. This fact means the discrepancies between the absolute values of different investigators are due to the differences in the calibration of the detection efficiency.

The emission cross sections by proton impact and helium ion impact are different in their energy dependence. In the case of helium ion impact, the energy dependence is steeper than that of proton impact. In the present energy region, the emission cross section by proton impact is due only to the "ionization process". The steeper energy dependence of helium ion impact, therefore, means that there are some contributions from the "charge transfer process" in this case. This conclusion is also supported by the comparison of the emission cross sections by proton and He^{2+} impacts with the same velocity. The emission cross section by a 2.0 MeV He^{2+} impact is about six times as large as that by a 500 keV proton impact. The predicted value of this ratio by the "ionization process" is 4, according to the z^2 -dependence of the cross section. Therefore, the difference between the experimental and predicted values must be attributed to the "charge transfer process".

Acknowledgement

The authors would like to express their sincere gratitude to Professor M. Sakisaka and Drs. M. Tomita, Y. Kido, N. Kobayashi and N. Maeda for their valuable discussions and continuous encouragement. Acknowledgement is also due to Mr. K. Norizawa for the design of the electroic devices. The authors are also grateful to Messrs. T. Ogawa, K. Tsumaki, A. Sawa and S. Andoh for their kind cooperation during the whole course of the present work.

References

- 1) E.W. Thomas; "Excitation in Heavy Particle Collisions," Wiley, New York, (1972).
- 2) R.H. Hughes and L.D. Weaver; Phys. Rev. **132**, 710 (1963).

- 3) R.M.St. John and C.C. Lin; J. Chem. Phys. **41**, 195 (1964). J. Chem. Phys. **47**, 347 (1967).
- 4) L.D. Weaver and R.H. Hughes; J. Chem. Phys. **47**, 346 (1967).
- 5) H.R. Moustafa Moussa and F.J. De Heer; Physica **36**, 646 (1967).
- 6) R.J. Anderson and R.H. Hughes; Phys. Rev. **A5**, 1194 (1972).
- 7) J.F. Sutton and R.B. Kay; Phys. Rev. **A9**, 697 (1974).
- 8) E.T.P. Lee and C.C. Lin; Phys. Rev. **138**, A301 (1965).
- 9) E.S. Gillespie; J. Phys. **B5**, 1916 (1972).
- 10) R.A. Mapleton; Phys. Rev. **109**, 1166 (1958).
- 11) R.A. Mapleton; Phys. Rev. **122**, 528 (1961).
- 12) R.H. Hughes, R.C. Waring and C.Y. Fan; Phys. Rev. **122**, 525 (1961).
- 13) J. Van Eck, F.J. De Heer and J. Kistemaker; Physica **28**, 1184 (1962).
- 14) J.G. Dodd and R.H. Hughes; Phys. Rev. **135**, A618 (1964).
- 15) E.W. Thomas and G.D. Bent; Phys. Rev. **164**, 143 (1967).
- 16) E.W. Thomas; Phys. Rev. **164**, 151 (1967).
- 17) M. Asari; Doctor Thesis, Kyoto University (1979).
- 18) V.S. Nikolaev, I.S. Dmitriev, L.N. Fateeva and Ya.A. Teplova; Sov. Phys. -JETP **13**, 695 (1961).
- 19) I.S. Dmitriev, V.S. Nikolaev, L.N. Fateeva and Ya.A. Teplova; Sov. Phys. -JETP **15**, 11 (1962).
- 20) L.I. Pivovarov, M.T. Novikov and V.M. Tuvaev; Sov. Phys. -JETP **15**, 1035 (1962).
- 21) P. Hvelplund and E.H. Pedersen; Phys. Rev. **A9**, 2434 (1974).
- 22) A. Itoh, M. Asari and F. Fukuzawa; J. Phys. Soc. Jpn **44**, 1672 (1978).
- 23) A. Itoh, M. Asari and F. Fukuzawa; Mem. Fac. Engng. Kyoto Univ. **39**, 201 (1977).
- 24) A. Itoh, M. Asari and F. Fukuzawa; Mem. Fac. Engng. Kyoto Univ. **39**, 321 (1977).